Boundary-Layer Meteorol (2014) 151:373–387
DOI 10.1007/s10546-013-9905-z

RESEARCH NOTE

# Intercomparison of Methods for the Simultaneous Estimation of Zero-Plane Displacement and Aerodynamic Roughness Length from Single-Level Eddy-Covariance Data

**Alexander Graf · Anneke van de Boer · Arnold Moene · Harry Vereecken**

Received: 2 May 2013 / Accepted: 31 December 2013 / Published online: 23 January 2014


**Abstract** We applied three approaches to estimate the zero-plane displacement $d$ through the aerodynamic measurement height $z$ (with $z = z_m - d$ and $z_m$ being the measurement height above the surface), and the aerodynamic roughness length $z_0$, from single-level eddy covariance data. Two approaches (one iterative and one regression-based) were based on the universal function in the logarithmic wind profile and yielded an inherently simultaneous estimation of both $d$ and $z_0$. The third approach was based on flux–variance similarity, where estimation of $d$ and consecutive estimation of $z_0$ are independent steps. Each approach was further divided into two methods differing either with respect to the solution technique (profile approaches) or with respect to the variable (variance of vertical wind and temperature, respectively). All methods were applied to measurements above a large, growing wheat field where a uniform canopy height and its frequent monitoring provided plausibility limits for the resulting estimates of time-variant $d$ and $z_0$. After applying, for each approach, a specific data filtering that accounted for the range of conditions (e.g. stability) for which it is valid, five of the six methods were able to describe the temporal changes of roughness parameters associated with crop growth and harvest, and four of them agreed on $d$ to within 0.3 m most of the time. Application of the same methods to measurements with a more heterogeneous footprint consisting of fully-grown sugarbeet and a varying contribution of adjacent harvested fields exhibited a plausible dependence of the roughness parameters on the sugarbeet fraction. It also revealed that the methods producing the largest outliers can differ between site conditions and stability. We therefore conclude that when determining $d$ for canopies with unknown properties from single-level measurements, as is increasingly done, it is important to compare the results of a number of methods rather than rely on a single

A. Graf (✉) · H. Vereecken
Agrosphere (IBG-3), Institute of Bio- and Geosciences, Jülich Research Centre, 52425 Jülich, Germany
e-mail: a.graf@fz-juelich.de

A. van de Boer
Meteorological Institute, University of Bonn, Bonn, Germany

A. van de Boer · A. Moene
Meteorology and Air Quality Department, Wageningen University, Wageningen, The Netherlands

one. An ensemble average or median of the results, possibly after elimination of methods that produce outliers, can help to yield more robust estimates. The estimates of $z_0$ were almost exclusively physically plausible, although $d$ was considered unknown and estimated simultaneously with the methods and results described above.

**Keywords** Aerodynamic roughness length · Barley · Eddy covariance · Sonic anemometer · Sugarbeet · Wheat · Zero-plane displacement

## 1 Introduction

objec-
tive
here
not
pheno!

The zero-plane displacement $d$ and aerodynamic roughness length $z_0$ are parameters of the logarithmic wind profile, and characteristic of the surface that are required in a multitude of meteorological modelling applications. Apart from larger-scale grid models (Garratt 1993), these include tasks frequently occurring during analyses of micrometeorological single-station data, such as estimation of the aerodynamic resistance (Blyth et al. 1993), frequency response correction to eddy-covariance fluxes (Moore 1986; Massman 2000), or footprint modelling (Schmid 1994).

Wait!
So
0.1H=
z0
only
applies
for zero
d?

Classically, both parameters are estimated from multi-level measurements of wind speed over a homogeneous surface (Lo 1976; Garratt 1978; de Bruin and Moore 1985; Kustas et al. 1989). This led to a body of literature summarizing values for different surfaces (Wieringa 1993). Those literature values can be used as an alternative if the above equipment and site conditions are not met. As a rule-of thumb, $d$ for a crop or forest canopy is considered 2/3 to 3/4 of the canopy height $h$, and $z_0$ about 10 % of canopy height in the absence of a non-zero $d$ (Foken 2008). Jacobs and van Boxel (1988) found $z_0 = 0.26(h - d)$ for a maize canopy. However, these rules of thumb should be modified if the surface of interest is not dense and uniform, in which case a site-specific determination is required (Kustas et al. 1989; Lloyd et al. 1992).

Through the eddy-covariance method, alternative possibilities of determining $d$ and $z_0$ have become available. Various authors report robust results if either several levels of sonic anemometer measurements, or one such level combined with a classic wind profile, is used to introduce direct knowledge of the friction velocity into the estimation procedure (Jacobs and van Boxel 1988; Weaver 1990; Lloyd et al. 1992; Takagi et al. 2003; Toda and Sugita 2003). At the same time, however, the eddy-covariance method to measure various fluxes has superseded the profile method, leaving many current stations without a wind-speed profile to enable the classic estimation of $d$ and $z_0$.

From single-level eddy-covariance measurements at one point in time, only one parameter can be estimated, usually $z_0$ while $d$ is assumed known. Even so, results tend to scatter considerably. It has been pointed out, however, that the use of multiple points in time providing different stability conditions can enable the estimation of both parameters if they are assumed constant over the time period regarded. These approaches either rely on flux–variance similarity (Weaver 1990; Rotach 1994; de Bruin and Verhoef 1997; Toda and Sugita 2003; Prueger et al. 2004) to estimate $d$ and consecutively $z_0$, or on the integrated universal function in the logarithmic wind profile to determine both simultaneously (Martano 2000; Gao and Bian 2004; Tsai et al. 2010). In both cases, iterations over the range of possible $d$ values are necessary.

Here, we extend these two approaches by a non-iterative, regression approach based on the flux–profile relationships. Each of the three approaches is represented by two implementations. The six resulting methods are compared to each other on two agricultural datasets.

No forest yet.

The first dataset represents a case where $z_0$ and $d$ vary in time due to crop development. In the second dataset the degree of heterogeneity varies between different measurement intervals. In this way, the methods can be tested for changing $d$ and $z_0$ values due to either crop growth or footprint variation.

## 2 Theory

### 2.1 Iterative Methods Based on Flux–Profile Similarity (FP-IT)

The wind profile in the surface layer is approximated by

$$\bar{u} = \frac{u_*}{\kappa}\left(\ln\frac{z}{z_0} - \Psi_m\left(\frac{z}{L}\right)\right), \tag{1}$$

where the overbar denotes time averaging, $\bar{u}$ is the average wind speed at the aerodynamic measurement height $z = z_m - d$, $z_m$ being the measurement height above the soil surface, $L$ and $u_*$ are the Obukhov length and the friction velocity, $\kappa$ is the von Karman constant (0.4) and $\Psi_m$ is the integrated universal momentum function, in which we neglect a small dependence on $z_0/L$, as is common. The Obukhov length is defined as,

$$L = -\frac{u_*^3 T_v \rho c_p}{\kappa g H_v}, \tag{2}$$

where $T_v$ is the virtual temperature, $g$ is the acceleration due to gravity (9.81m s$^{-2}$), $\rho c_p$ is the volumetric heat capacity at constant pressure (with $c_p = 1{,}005\,\mathrm{J\,kg^{-1}\,K^{-1}}$), and $H_v$ is the the buoyancy (virtual heat) flux. Here we approximate $H_v$ and $T_v$ by the heat flux and mean temperature based on the sonic temperature. Using variables based on the sonic temperature has the advantage that no additional humidity sensor (with possible failures) is needed. $\Psi_m$ is most commonly described as

$$\Psi_m\left(\frac{z}{L}\right) = \ln\left(\frac{1+x^2}{2}\left(\frac{1+x}{2}\right)^2\right) - 2\arctan x + \frac{\pi}{2} \tag{3}$$

for $z/L < 0$ with

$$x = \left(1 - \gamma\frac{z}{L}\right)^{\frac{1}{4}} \tag{4}$$

for unstable conditions (Paulson 1970), where $\gamma$ is a universal constant depending on $\kappa$ and on experimental evidence and is approximated by 19.3 (Högström 1988). For moderately stable conditions

$$\Psi_m\left(\frac{z}{L}\right) = -\beta\frac{z}{L} \tag{5}$$

($0 < z/L < 1$), where $\beta = 6$ is another universal constant. For $z/L$ near and above 1, this is less well established since a decrease of $\beta$ with further increasing $z/L$ has been suggested by some (Holtslag and de Bruin 1988; Handorf et al. 1999; for an overview see Foken 2008).

If $d$ (and thus $z$) is known, $z_0$ can be estimated from a single set of $\bar{u}$, $u_*$, and $L$ obtained from a single-level eddy-covariance station by rearranging Eq. 1,

what about the wind speed class issue? why did that seem to be important for my calc.

$$z_0 = \frac{z}{\exp\left(\frac{\bar{u}\kappa}{u_*} + \Psi_m\left(\frac{z}{L}\right)\right)}, \tag{6}$$

Ans: Artifact of stability?

where averaging across multiple points in time can be used to yield more robust results ($\overline{z_0}$), and the standard deviation $\sigma_{z_0}$ can be used to quantify the uncertainty of the estimate. Martano (2000) provided mathematical evidence that an unknown $d$ can be estimated iteratively by repeating this procedure for a large range of possible $z$ values and selecting the results where the standard deviation of a parameter $S$, $\sigma_S$, becomes minimal, with either

Could us fmincon in Matlab or python equivalent

$$\sigma_S = \sigma\left(\frac{\bar{u}\kappa}{u_*} + \Psi_m\left(\frac{z}{L}\right)\right) \tag{7}$$

or the approximation

$$\sigma_S \approx \frac{\sigma_{z_0}}{\overline{z_0}}. \tag{8}$$

Largest systematic devs from plaus. range

Estimation of $z$ and $z_0$ using Eq. 7 or 8 will be referred to as FP-IT-1 and FP-IT-2, respectively.

## 2.2 Regression Methods (FP-RE)

The need for iteration in FP-IT is a result of the non-trivial non-linearity in $\Psi_m$. Therefore, in this section we develop a simple modification that relies on its approximate linearity within a certain stability range. Restricting the data to this range enables the use of linear regression to determine $d$ and $z_0$. For various other purposes, the same type of equation has already been suggested by Monin and Oukhov (1954) for the range $|z/L| < 1$, based on a power series expansion of the then unknown universal function truncated after the linear term (their Eq. 43). The current integrated universal functions (Eqs. 3 and 5) suggest an asymmetric validity range of such a simplification, since exact linearity is typically assumed in the range $0 < z/L < 1$, whereas for $z/L < 0$ the function is non-linear (the applicability of a linearity assumption near neutral conditions will be discussed in Sect. 3.3). Inserting Eq. 5 into Eq. 1, we obtain

$$\bar{u} \approx \frac{u_*}{\kappa}\left(\ln\frac{z}{z_0} + \beta\frac{z}{L}\right). \tag{9}$$

Now, for multiple points in time with varying $\bar{u}$, $u_*$ and $L$, we can set up linear regression models with two parameters $a$ and $b$, where $z$ can be estimated directly from the regression coefficient $b$, and $z_0$ from $b$/exp($a$). First we consider a simple linear regression with an offset parameter and a slope parameter,

$$\frac{\bar{u}\kappa}{u_*} = a + b\frac{\beta}{L} \tag{10}$$

where the left-hand side is the dependent variable and $\beta/L$ is the regressor. To test the sensitivity on model choice, we additionally use a multiple linear regression without offset,

$$\bar{u} = a\frac{u_*}{\kappa} + b\frac{u_*\beta}{\kappa L}, \tag{11}$$

where $\bar{u}$ is the dependent variable and the expressions following $a$ and $b$ are the two regressors. Estimation of $z$ and $z_0$ using Eq. 10 or 11 will be referred to as FP-RE-1 and FP-RE-2, respectively.

## 2.3 Flux–Variance Methods (FV)

An independent approach uses flux–variance similarity (Weaver 1990; Rotach 1994; Toda and Sugita 2003). Iteratively changing $z$, the (root-)mean-square difference between the left-hand side and the right-hand side of one or both of the following equations is minimized,

These methods thus harder to implement b/c they include devs

$$\frac{\sigma_w}{u_*} = C_1 \left(1 - C_2 \frac{z}{L}\right)^{\frac{1}{3}}, \tag{12}$$

where $\sigma_w$ is the standard deviation of the vertical wind velocity, and $C_1$ and $C_2$ are universal constants, and

$$\frac{\sigma_{Tv}}{T_{*v}} = -C_3 \left(C_4 - \frac{z}{L}\right)^{-\frac{1}{3}}, \tag{13}$$

where $\sigma_{Tv}$ is the standard deviation of virtual temperature, and $T_{*v} = -\overline{w'T_v'}/u_*$. For the universal constants we use $C_1 = 1.3$, $C_2 = 2.0$ (Panofsky et al. 1977), $C_3 = 0.99$ and $C_4 = 0.06$ (see Toda and Sugita 2003). Estimation of $z$ using Eq. 12 or 13 will be referred to as FV-IT-1 and FV-IT-2, respectively. A regression-based approach for $z$ has also been suggested for flux–variance similarity, based on the free convection limit of Eqs. 12 and 13 (de Bruin and Verhoef 1997; Zhang and Park 1999; de Franceschi et al. 2009). On our dataset, however, it yielded strongly fluctuating results not included in the further comparison. Unlike the flux–profile approaches, the flux–variance approach estimates $z$ (and thus $d$) alone, without an inherent simultaneous determination of $z_0$. The latter can be added as an independent step, using e.g. Eq. 6. By combining flux–variance with flux–profile similarity in neutral conditions, another approach has been suggested to estimate $z_0$ from $\sigma_w$, $\bar{u}$ and an already known $z$ (Panofsky 1984),

$$\sigma_w = \frac{\kappa C_1}{\ln\left(\frac{z}{z_0}\right)} \bar{u} \tag{14}$$

for $z/L \approx 0$. Solving directly for $z_0$ shows that this approach is identical to the neutral limit of Eq. 6 except for the estimation of $u_*$ by $\sigma_w$ and $C_1$. Here, however, we follow Panofsky (1984) in using the regression of $\sigma_w$ against $\bar{u}$ to estimate the proprtionality factor and from that $z_0$. Because both Eqs. 14 and 12 use $\sigma_w$, we will here refer to Eq. 14 as an extension of FV-IT-1 to estimate $z_0$.

An overview of all methods is given in Table 1.

**Table 1** Overview of the compared methods to determine roughness parameters

| Name | Result | Solution method | Selection criteria |
|---|---|---|---|
| FP-IT-1 | $z_0$ and $d$ | Cost function (Eqs. 6, 7) | $\bar{u} > 1.5$ m s$^{-1}$, $-0.084 < \frac{z_{0\,max}}{L} < 0.037$, $\frac{z_{max}}{L} < 1$ |
| FP-IT-2 | $z_0$ and $d$ | Cost function (Eqs. 6, 8) | $\bar{u} > 1.5$ m s$^{-1}$, $-0.084 < \frac{z_{0\,max}}{L} < 0.037$, $\frac{z_{max}}{L} < 1$ |
| FP-RE-1 | $z_0$ and $d$ | Regression (Eqs. 9, 10) | $-0.084 < \frac{z_{0\,max}}{L} < 0.037$, $-0.103 < \frac{z_{max}}{L} < 1$ |
| FP-RE-2 | $z_0$ and $d$ | Regression (Eqs. 9, 11) | $-0.084 < \frac{z_{0\,max}}{L} < 0.037$, $-0.103 < \frac{z_{max}}{L} < 1$ |
| FV-IT-1 | $z_0$ and $d$ | Cost function (Eq. 12) for $d$, Regression (Eq. 14) for $z_0$ | for $d$: $u_* > 0.05$ m s$^{-1}$ and $T_* < -0.3$ K<br>for $z_0$: $\bar{u} > 1.5$ m s$^{-1}$ and $\lvert z/L \rvert < 0.4$ |
| FV-IT-2 | $d$ | Cost function (Eq. 13) | $u_* > 0.05$ m s$^{-1}$ and $T_* < -0.3$ K |

## 3 Material and Methods

### 3.1 Dataset

We use eddy-covariance measurements carried out at several stations in a flat landscape dominated by a mosaic of winter wheat, sugarbeet and winter barley fields in 2009 (Graf et al. 2010; Boer et al. 2013). Here, we mainly focus on the measurement that provided the most uniform footprint over a prolonged time period. These data are confined to heights of 2.4 m (2.6 m until May 5) above the soil surface of a winter wheat field 380 m by 190 m wide, surrounded by a large portion of further winter wheat fields. Weekly manual observations of canopy height by ourselves and another group (Korres et al. 2013) indicated a linear ($r^2 > 0.95$) growth from the start of the eddy-covariance measurements (0.30 m at April 24) until July 1, followed by stagnation (1.0 m) until harvest at August 4. Measurements continued on the bare site until August 28.

The data required here rely on the sonic anemometer (CSAT3, Campbell Scientific, Logan, UT, USA) logged at 20 s$^{-1}$. Averages, (co)variances and fluxes were computed over 30-min time blocks using the software ECpack (van Dijk et al. 2004). The scheme included the elimination of raw data points flagged by the instrument, linear detrending, and the planar fit method (Wilczak et al. 2001). The time periods over which planar fit angles were determined were defined by the station maintenance dates, which included the option to readjust the guy wiring (typically between 5 and 12 days). The usual correction of sonic temperature (Schotanus et al. 1983) was not performed for this study, in order to match the definition of $L$ given in Eq. 2.

will need to back out sonic temp.

A footprint model (following section) was used to eliminate sub-periods where the measurements were dominated by other crops in the surrounding. After the barley and wheat fields of the area had been harvested, a second station in a smaller (310 m by 170 m) sugarbeet field provided the opportunity to test the sensitivity of the methods to varying contributions of bare soil ($d \approx 0$) and sugarbeet to the footprint (sugarbeet having an approximately stagnant canopy height of 0.68 m by then). The sonic anemometer, identical in type, logging and processing, was positioned 2.48 m above the soil surface; measurements at this site continued until the harvest of the sugarbeet on September 30.

### 3.2 General and Footprint-Based Data Filtering

To exclude erroneous data, we first defined lower and upper limits for a number of micrometeorological quantities resulting from the processing. ECpack computes estimates of the 95 % confidence interval for each average and flux, based on the standard error of moments (Kendall and Stuart 1958; Moene and Michels 2002; van Dijk et al. 2004; Graf et al. 2010). Plots of the confidence interval against the the quantity under consideration exhibited an approximately linear relationship with increasing errors for larger values, in good agreement with other studies (see Kessomkiat et al. 2013 for an overview). We defined an upper limit to the permissible 95 % confidence interval of 0.2 m s$^{-1}$ $+0.004\,\bar{u}$ for $\bar{u}$, of 0.05 m s$^{-1}$ $+0.0025|\bar{w}|$ for the mean vertical velocity component $\bar{w}$, of 0.2 m s$^{-1}$ $+0.1\,u_*$ for $u_*$, and of 25 W m$^{-2}$ $+0.075|H_v|$ for the buoyancy flux $H_v$. The confidence intervals of virtual temperature $T_v$ and wind direction did not scale with the mean values and were limited to 0.1 K and 180°, respectively. For $|H_v|$ and $u_*$, additional limits to the variable itself were established of 1,000 W m$^{-2}$ and 1 m s$^{-1}$, respectively. In a software intercomparison, it was found that this exclusion scheme proved similar to only retaining "zero flags" according to the Spoleto agreement as implemented in the TK2 software (Mauder and Foken 2004).

Will I need to worry bout foot-print

To exclude situations dominated by other crops in the case of the wheat data, and to quantify the contribution of other crops in the case of the sugarbeet data, the footprint model described in detail by van de Boer (2013, version RefHKC-KM, cf. Hsieh et al. 2000; Kormann and Meixner 2001) was used. To prevent any effect of more distant surface types with radically different $z_0$ or $d$ values, such as a lake, trees, buildings or maize, we first eliminated from both datasets all situations with less than 90 % cumulative contribution of the wheat, barley and sugarbeet fields of the study area. For the wheat dataset, we additionally excluded all situations with less than 50 % wheat contribution.

In order to determine $d$ and $z_0$ estimates as a function of time for the wheat dataset, we applied a running window to the time series that advanced one day at a time. Only data within this window are used to compute the cost function (FP-IT, FV-IT) or regression (FP-RE) from which $d$ and $z_0$ for the respective day are estimated. As a trade-off between the need for a large sample size on the one hand, and the risk of ignoring intrinsic changes of $d$ and $z_0$ on the other hand, we chose a length of the running window of 31 days, i.e. including 15 days before and 15 days after the day for which the roughness parameters are determined. The window was not allowed to cross the date of harvest. Each of the six methods was applied to each running window position; for the iterative methods $d$ was varied in steps of 0.1 m.

one month is very course

For the heterogeneous (sugarbeet) dataset, $d$ and $z_0$ of the two involved surface types bare (harvested) and sugarbeet were considered constant in time, but their effective value for the station was assumed to be a function of the footprint. Consequently, the running window was applied to the sugarbeet contribution in this analysis. Again as a trade-off between sample size and precision, a running window size of 50 % sugarbeet contribution was chosen.

The result of each method for each position of the running window was only considered valid, if after the above filters and those described in the following section, at least 30 half-hourly records were available.

### 3.3 Method-Specific Data Filtering

Each of the methods described in Sect. 2 is subject to different limitations, in particular with respect to the stability range over which they are applicable. The first four methods are based on the published analytical solutions (Eqs. 3–5) for $\Psi_m$, which neglect the lower integration bound $z_0/L$. In this way considerable computational effort to scan the whole space of possible $z_0$ and $d$ combinations for an optimum is prevented. Although this simplification is common practice in other research topics, we have no knowledge of the effect of this simplification on the $z_0$ estimation, apart from an empirical finding by Martano (2000): the two methods FP-IT-1 and FP-IT-2, in combination with a wind speed filter ($\bar{u} > 1.5\,\mathrm{m\,s^{-1}}$), compared well with a method that does not ignore the lower integration bound. To quantify the errors to be expected from the simplification, we go back to Eq. 6 and replace $\Psi_m(z/L)$ by $\Psi_M(z/L) \approx \Psi_m(z/L) - \Psi_m(z_0/L)$, $\Psi_M$ being the theoretically exact integral and $\Psi_m$ the usual solution (Eqs. 3–5). Starting from the ratio between both versions of Eq. 6, it can be shown that the relative systematic error in the $z_0$ estimate is

$$\frac{\Delta z_0}{z_0} = \left|1 - \exp\left(-\Psi_m\left(\frac{z_0}{L}\right)\right)\right|. \tag{15}$$

Allowing for a relative error of 25 % yields a condition

$$-0.084 < \frac{z_{0\,\max}}{L} < 0.037 \tag{16}$$

for methods FP-IT-1 and FP-IT-2, where $z_{0\max}$ is an upper bound to the expected $z_0$ values (e.g. $0.1h$). It should be noted that the resulting accuracy in $d$, through the iteration process and the different cost functions Eqs. 7 and 8, cannot be tracked with the same simple means. It will additionally show a slight dependence on $\bar{u}\kappa/u_*$. Also, the propagation of random errors in all input variables is ignored here. We hypothesize that the empirical data selection criterion $\bar{u} > 1.5$ m s$^{-1}$ originally proposed by Martano (2000), acts to limit most of these error sources at once. Here, we apply both, the wind speed threshold and Eq. 16 (with $z_{0\max} = 0.1$ m).

Methods FP-RE-1 and FP-RE-2 are subject to additional stability limitations. There are two approaches to justifying the linear Eq. 9 and determining its coefficient $\beta$. In the range $0 < z/L < 1$, the most widespread set of $\Psi_m$ functions assumes the linear Eq. 9 to hold exactly, and $\beta = 6$. Another approach was already used by Monin and Oukhov (1954) to discuss the effects of stability on various parameters in the near-neutral range. At the time no expression for $\Psi_m$ existed, but it was expected that it could be described by a Taylor series expansion at the point $z/L = 0$. Truncating the expansion after the linear term led to an approximation with only one unknown parameter ($\beta$). The valid stability range of this simplification was given arbitrarily as $|z/L| < 1$. The current usual version of $\Psi_m$ (Eqs. 3–5) suggests that in this case $\beta$ should be replaced by a compromise between the stable value 6 and a slightly smaller value for unstable conditions, which would be either the asymptotic derivative of $\Psi_m$ for $z/L \to 0$, or a mean slope over a predetermined range. We use a mixed approach: it acknowledges the fact that stable conditions provide the best justification for a linearity assumption and also contribute most to the variance in $\Psi_m$, but it extends into the slightly unstable range. Using $\beta = 6$, a limit to negative $z/L$ values can be derived from the difference between the "true" unstable universal function (Eq. 3), and its approximation by the extrapolated stable function (Eq. 5). For consistency with the above procedure for method FP-IT, we consider the importance of this difference again in the framework of Eq. 6, although it is not explicitly used in this form by method FP-RE,

$$\frac{\Delta z_0}{z_0} = \left|1 - \exp\left(\Psi_m\left(\frac{z}{L}\right) - \beta\frac{z}{L}\right)\right|. \tag{17}$$

Again, allowing for a 25 % error in $z_0$ (which will take the form of an underestimation), the additional condition for method FP-RE is

$$-0.103 < \frac{z_{\max}}{L} < 1, \tag{18}$$

where $z_{\max}$ is an upper bound to the expected $z = z_m - d$ values, e.g. $z_m$, and the stable (right) limit is based on the assumption that the shape of $\Psi_m$ is unknown for $z/L > 1$. Note that this last limitation equally applies to the FP-IT methods.

The flux–variance approach also has limitations. In agreement with Prueger et al. (2004),who found that $d$ values from this method were frequently unrealistic, we could establish a sufficient robustness for this method only under multiple constraints. We confine analysis with these equations to unstable situations, and exclude situations where the quantities in the denominator of the left-hand sides approach zero (i.e. where $u_* < 0.05$ m s$^{-1}$ and $T_* > -0.3$ K). For the consecutive determination of $z_0$ following Panofsky (1984) in method FV-IT-1, neutral conditions and strong winds are required; here we use the same wind-speed threshold as for FP-IT-1 and FP-IT-2 methods ($\bar{u} > 1.5$ m s$^{-1}$), and $|z/L| < 0.4$ to limit the importance of the stability factor in Eq. 12 to 25 %, where $z$ is the already known estimate from application of the first part of method FV-IT-1.

## 4 Results and Discussion

### 4.1 Growth Stages of a Uniform Wheat Canopy

Figure 1 provides the estimates of the aerodynamic measurement height $z$, the aerodynamic roughness length $z_0$, and the number of half-hourly records passing the quality control for the temporal changes in the wheat canopy. For comparison, a physically plausible range of $z$ is shown as the shaded area, assuming $z_m - h < z < z_m - 0.5h$. For the post-harvest state, we inserted $h = 0$ on the left-hand side and $h = 0.1$ m on the right-hand side of this inequality, in order to account for any possible displacement effects by the freshly grubbed soil.

All methods based on flux–profile similarity reflect the expected seasonal course of the aerodynamic measurement height $z$, with a decrease during the growth period, approximate stagnation afterwards and a clear increase after the harvest. The flux–variance methods show only a small sensitivity to the crop height change after harvest; this applies especially to the temperature-based version (FV-IT-2) which also most poorly reflects the growth and stagnation period. In terms of absolute accuracy, the largest systematic deviations from the plausibility range occur with method FP-IT-2 during the early and late periods of low (or no) canopy height. Then high $z$ estimates above $z_m$ occur, implying negative $d$ values. With method FV-IT-2, on the other hand, during most of the measurement period low $z$ estimates imply $d$ values considerably larger than the canopy height. The poorer performance of method FP-IT-2 as compared to FP-IT-1 is in agreement with the more strict derivation of the latter, as well as with empirical findings of Martano (2000).

The remaining estimates and the median of all estimates are mostly within <0.3 m of each other and of the plausibility range. Given the fact that no knowledge about $z_m$ is used in the methods (apart from the global $z_{\max}$ parameter used exclusively to determine the stability thresholds described in Sect. 3.3), all methods perform well in estimating the measurement height from turbulence statistics. In practical applications, however, $z_m$ is known and $d$ is the unknown of interest. For $d \leq 1$ m uncertainties of 0.5 m translate into relative errors larger than 50 %. Thus for simple, well-defined crop surfaces such as those studied here, a determination of $d$ from $h$ using the rule-of-thumb would be preferable. If $h$ is not known or if the canopy is more complex, and the accuracy of consecutive model applications only depends on the relative accuracy of $z$, determination from single-level eddy-covariance measurements would still be an option. In the following section, we test whether the compared methods perform similarly in more heterogeneous conditions.

Estimates of the aerodynamic roughness length (Fig. 1b) also show a plausible relative course over the season, following changes in canopy height. Only method FP-IT-2 fails to exhibit a clear reduction after the harvest. The shaded plausibility area for $z_0$ is only defined by an upper limit $z_{0\max} = 0.15h$ (compare with Raupach 1994), and only for periods where a canopy was present. All of the methods match the plausibility limits most of the time. Since $z_0$ can be less well confined than $d$ by physical plausibility considerations, a practical option for the characterization of poorly known canopies is to estimate $d$ conventionally (as a fixed portion of the canopy height), and then determine $z_0$ from turbulence statistics (e.g. using Eq. 6 or 14). This approach, which may be considered an intermediate solution between determining both $d$ and $z_0$ from turbulence statistics and estimating both from canopy height and the rule-of-thumb, has, e.g., been used for footprint modelling by Neftel et al. (2008) and van de Boer et al. (2013).

The sample sizes $N$ (Fig. 1c) underline the fact that the three approaches build on different parts of the datasets of half-hourly records representing conditions where the underlying

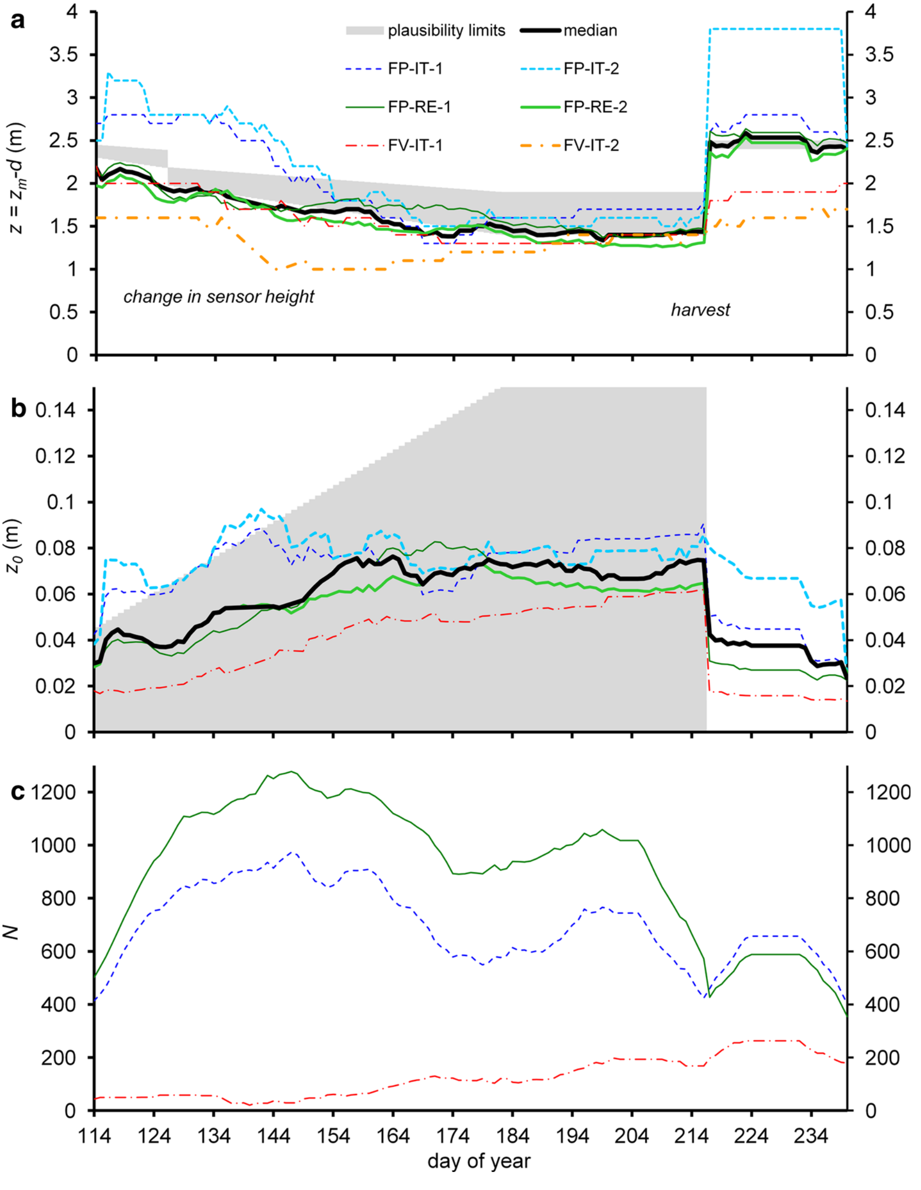


**Fig. 1** Seasonal course of estimated aerodynamic measurement height $z$ (**a**) and aerodynamic roughness length $z_0$ (**b**) of a wheat canopy after applying a 1-day binning and a 31-day running window to the estimation methods as identified in Sect. 2. **c** The number of half-hourly records in the window available after the particular data filtering of each method; this is identical for the two sub-methods of each of the approaches FP-IT, FP-RE and FV-IT

assumptions of each particular approach are valid. Method FP-RE relies on stable and near-neutral situations, which were met more frequently in the first half of the measurement period when the wheat canopy was still green and the Bowen ratio lower during the day. Method FV-IT, in contrast, relies on unstable situations and received its maximum sample size after the harvest. Flux–variance methods generally excluded more data than flux–profile methods in our dataset. However, while apparently depending more heavily on data quality than flux–profile methods, $z(d)$ estimation by flux–variance methods also depends less heavily on large sample sizes. The reason is that Eqs. 12 and 13 can theoretically be solved with a single half-hourly record of turbulence statistics, whereas all flux–profile methods require variation in stability for a unique solution. The fact that each approach builds on different data might explain a part of the differences between the approaches, which are slightly larger than the differences between the two sub-methods of each approach (see Fig. 1a). It is an underlying assumption of Eq. 1, that $z_0$ and $d$ are independent of stability; therefore the different methods should ideally lead to identical results although they use different stability ranges of the dataset. The differences in results may indicate that in fact $z_0$ and $d$ are not perfectly independent of stability. Harman and Finnigan (2007) state that the independence assumption might become increasingly invalid when approaching the roughness sublayer.

### 4.2 Relation to Canopy Height

If z too close to canopy, a problem...

Figure 2 shows the dependence of the ensemble medians of the zero-plane displacement $d$ and the aerodynamic roughness length $z_0$ on canopy height $h$ during the growth phase. The slope of the relation of $d$ against $h$, 0.82, is somewhat higher than expectations from the rule-of-thumb (0.67–0.75) and the one of $z_0$ against $h$, 0.06, somewhat lower (0.10). This deviation might be an artefact since Fig. 1 indicates that methods yielding highest $d$ estimates typically yield the lowest $z_0$ estimates, and vice versa. However, both values match ratios modelled by Raupach (1994) and Massman (1997) for very dense canopies with a canopy area index $>1$.

Alternatively, $z_0$ can be described as a fraction of $h - d$ (Jacobs and van Boxel 1988). Depending on whether we use the instantaneous median $d$ estimate, model $d$ with the $d/h$ ratio of 0.82 derived from Fig. 2, or use a more conservative estimate of 0.75, the regression-based ratio $z_0/(h-d)$ varies between 0.11 and 0.34. This is in rough agreement with a value of 0.26 reported for maize by Jacobs and van Boxel (1988).

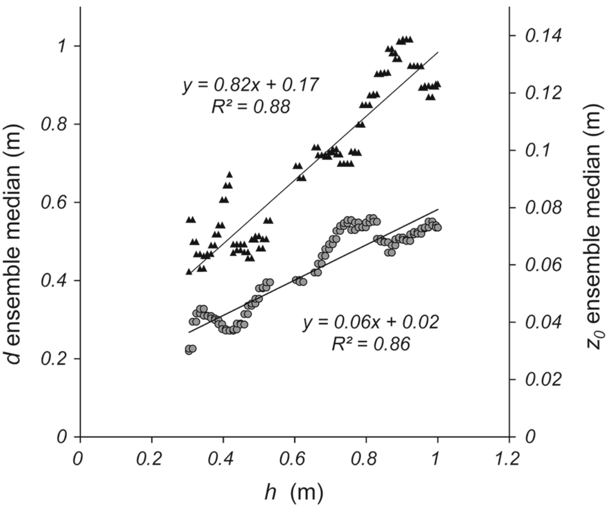


**Fig. 2** Zero-plane displacement $d$ (*triangles*) and aerodynamic roughness length $z_0$ (*circles*) from Fig. 1 as a function of measured canopy height during wheat growth

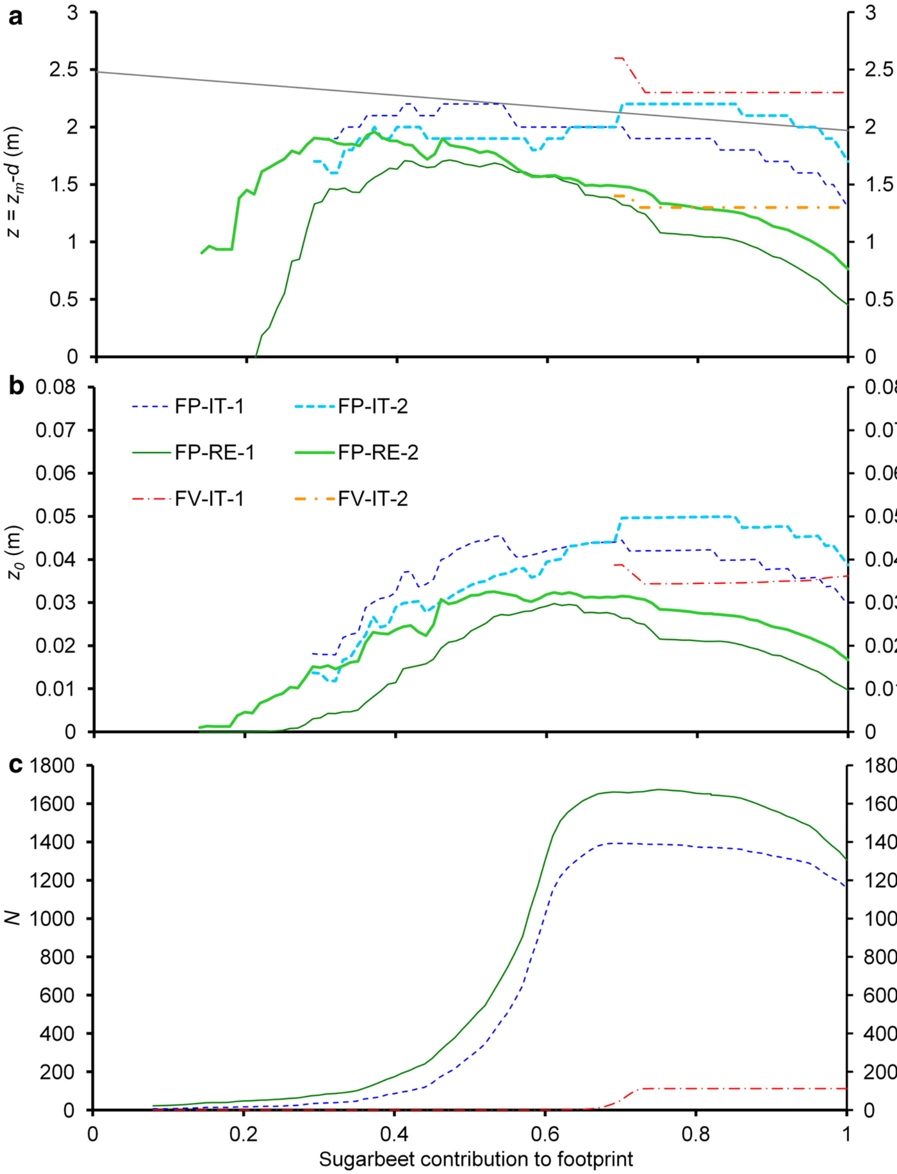


**Fig. 3** Estimated aerodynamic measurement height $z$ (**a**) and aerodynamic roughness length $z_0$ (**b**) of a station in a sugarbeet field during a period of approximately constant canopy height, as a function of sugarbeet contribution (as opposed to the contribution of surrounding bare soil fields) to the modelled station footprint. Running window width is 0.5. **c** The number of half-hourly records in the window available after the particular data filtering of each method

## 4.3 Extensibility to Heterogeneous Canopies

Section 4.1 suggests that in uniform, dense canopies determination of $d$ from turbulence statistics is not advantageous over rule-of-thumb estimates. Indeed method FP-IT and method

FV-IT have typically been used in situations where the canopy was difficult to characterize, such as buildings and tree groups interspersed with open areas (e.g. Rotach 1994; Martano 2000; Toda and Sugita 2003). Usually there is no reliable reference to validate the estimates in such conditions, and our findings from Sect. 4.1 are only transferable if heterogeneity itself does not affect too severely the validity of the used functions, all of which are based on MOST and thus implicitly assume homogeneity. Figure 3 shows the $z$ and $z_0$ results of the different methods when applied to a station in a sugarbeet field, with various footprint contributions by surrounding bare fields (see Sects. 3.1 and 3.2).

An auxiliary line in Fig. 3a depicts the theoretical decline in the effective value of $z$ that would be expected from linear interpolation between $d = 0$ on the surrounding bare (harvested) fields and $d = 0.75h$ on the sugarbeet field. The slope of this line is approximately matched by the method FP-IT-1, method FP-RE-1 and method FP-RE-2 between about 30 % and 90 % sugarbeet contribution. Smaller and higher sugarbeet contributions were strongly linked to low sample sizes (Fig. 1c), which occurred in this type of analysis together with extreme stability conditions: The highest sugarbeet contributions were linked with the most unstable conditions favouring the smallest extension of the modelled footprint, and vice versa. This presumably invalidated the application of all flux–profile methods; as discussed in Sect. 4.1, they require a range of varying stability conditions.

Inside the range where all flux–profile methods exhibit a plausible decrease of $z$ with increasing sugarbeet contribution, the absolute magnitude of $z$ is underestimated by approximately zero (method FP-IT-2) to almost 1 m (method FP-RE-1). The fact that method FP-IT yields the most plausible absolute magnitude here and in the fully grown stage of Fig. 1, but led to considerable overestimations in another situation (Sect. 4.1), demonstrates that no single method is superior; rather, careful comparison of all methods can help to define an uncertainty range. The flux–variance methods, due to their association with unstable conditions, only yield estimates for situations where the modelled footprint is small and thus the sugarbeet contribution already is high; they add little to understanding the effect of varying contributions by bare soil. However, they provide a reasonable extrapolation into a stability range where flux–profile methods cannot yield meaningful results any more.

Similar observations apply to the aerodynamic roughness length (Fig. 1b), which increases with increasing sugarbeet contribution. The effective mixing of aerodynamic roughness lengths is known to be non-linear (Foken 2008), which is at least rudimentarily reflected by the curvature of all flux–profile methods. However, again flux–profile estimates below 30 % and above 90 % sugarbeet contribution are probably artifacts.

## 5 Conclusions

We applied three approaches for estimating the zero-plane displacement (from the aerodynamic measurement height) and aerodynamic roughness length from single-level eddy-covariance data. Each approach was represented by two methods and tested at two sites. One site was homogeneous, and the two parameters were expected to change with time due to canopy growth and harvest. The second was a more heterogeneous site where the parameters were expected to change with changing crop mixture in the station footprint. Most methods yielded relative changes of roughness parameters that were in line with expectations from changes of the canopy height within the footprint. However, each method showed temporary deviations from the other methods and from plausibility limits, depending on site and atmospheric conditions. To yield estimates that can approximately compete with the rule-of-thumb in dense, uniform canopies, it is therefore important not to rely on a single published method, but combine a number of them and compare them. The median of the six methods used here appears to perform well. For more irregular or poorly described canopies the rule-of-thumb does not apply and the above mentioned combination of methods can provide useful information on the uncertainty range of roughness parameters, provided that they are handled with care. Code for this application (MATLAB™ / GNU OCTAVE) can be obtained from the authors.

**Acknowledgments** This study was enabled by the Deutsche Forschungsgemeinschaft (DFG) in the framework of the project "Links between local scale and catchment scale measurements and modelling of gas exchange processes over land surfaces" (GR2687/3-1 and SCHU 2350/2-1). Additional synergies were provided by the Helmholtz investment initiative TERENO (instrument availability) and the DFG Collaborative Transregional Research Centre 32 "Patterns in Soil–Vegetation–Atmosphere–Systems", particularly subproject C3, which provided their canopy-height measurements for comparison and densification of our own observations. We would like to thank Martin Lennefer, University of Bonn, and Bernhard Pospichal, now University of Leipzig, for assistance in the set-up and regular maintenance of the stations, and Dirk Schüttemeyer, University of Bonn (now European Space Agency) for support in the set-up as well as helpful comments on the manuscript. We are indebted to the three anonymous reviewers for suggestions that helped to greatly improve the manuscript.

## References

Blyth EM, Dolman AJ, Wood N (1993) Effective resistance to sensible- and latent-heat flux in heterogeneous terrain. Q J R Meteorol Soc 119:423–442

de Bruin HAR, Moore CJ (1985) Zero-plane displacement and aerodynamic roughness length for tall vegetation, derived from a simple mass conservation hypothesis. Boundary-Layer Meteorol 31:39–49

de Bruin HAR, Verhoef A (1997) A new method to determine the zero-plane displacement. Boundary-Layer Meteorol 82:159–164

de Franceschi M, Zardi D, Tagliazucca M, Tampieri F (2009) Analysis of second-order moments in surface layer turbulence in an Alpine valley. Q J R Meteorol Soc 135:1750–1765

Foken T (2008) Micrometeorology. Springer, Heidelberg, 308 pp

Garratt JR (1978) Flux profile relations above tall vegetation. Q J R Meteorol Soc 104:199–211

Garratt JR (1993) Sensitivity of climate simulations to land-surface and atmospheric boundary-layer treatments—a review. J Clim 6:419–449

Gao Z, Bian L (2004) Estimation of aerodynamic aerodynamic roughness length and zero-plane displacement of an urban surface from single-level sonic anemometer data. Aust Meteorol Mag 53:21–28

Graf A, Schüttemeyer D, Geiß H, Knaps A, Möllmann-Coers M, Schween JH, Kollet S, Neininger B, Herbst M, Vereecken H (2010) Boundedness of turbulent temperature probability distributions, and their relation to the vertical profile in the convective boundary layer. Boundary-Layer Meteorol 134:459–486

Högström U (1988) Non-dimensional wind and temperature profiles in the atmospheric surface layer: a re-evaluation. Boundary-Layer Meteorol 42:55–78

Holtslag AAM, de Bruin HAR (1988) Applied modelling of the nighttime surface energy balance over land. J Appl Meteorol 27:689–704

Harman IN, Finnigan JJ (2007) A simple unified theory for flow in the canopy and roughness sublayer. Boundary-Layer Meteorol 123:339–363

Hsieh C, Katul G, Chi T (2000) An approximate analytical model for footprint estimation of scalar fluxes in thermally stratified atmospheric flows. Adv Water Resour 23:765–772

Handorf D, Foken T, Kottmeier C (1999) The stable atmospheric boundary layer over an Antarctic ice sheet. Boundary-Layer Meteorol 91:165–186

Jacobs AFG, van Boxel JH (1988) Changes of the zero-plane displacement and aerodynamic roughness length of maize during the growing season. Agric For Meteorol 42:53–62

Kormann R, Meixner FX (2001) An analytical footprint model for non-neutral stratification. Boundary-Layer Meteorol 99:207–224

Kessomkiat W, Hendricks Franssen HJ, Graf A, Vereecken H (2013) Estimating random errors of eddy covariance data: an extended two-tower approach. Agric For Meteorol 171–172:203–219

Kendall MG, Stuart A (1958) The advanced theory of statistics: distribution theory, vol 1. Griffin, London, 431 pp

Kustas WP, Choudhury BJ, Kunkel K, Gay LW (1989) Estimate of the aerodynamic roughness parameters over an incomplete canopy cover of cotton. Agric For Meteorol 46:91–105
Korres W, Reichenau TG, Schneider K (2013) Patterns and scaling properties of surface soil moisture in an agricultural landscape: an ecohydrological modelling study. J Hydrol 498:89–102
Lo AK (1976) An analytical-empirical method for determining the aerodynamic roughness length and zero-plane displacement. Boundary-Layer Meteorol 12:141–151
Lloyd CR, Gash JHC, Sivakumar MVK (1992) Derivation of the aerodynamic roughness parameters for a Sahelian savannah site using the eddy correlation technique. Boundary-Layer Meteorol 58:261–271
Massman WJ (1997) An analytical one-dimensional model of momentum transfer by vegetation of arbitrary structure. Boundary-Layer Meteorol 83:407–421
Moore CJ (1986) Frequency response corrections for eddy correlation systems. Boundary-Layer Meteorol 37:17–35
Martano P (2000) Estimation of surface aerodynamic roughness length and zero-plane displacement from single-level sonic anemometer data. J Appl Meteorol 39:708–715
Massman WJ (2000) A simple method for estimating frequency response corrections for eddy covariance systems. Agric For Meteorol 104:185–198
Mauder M, Foken T (2004) Documentation and instruction manual of the eddy covariance software package TK2. Arbeitsrgebnisse Univ, Bayreuth, Abt. Mikrometeorologie, Nr. 26
Moene AF, Michels BI (2002) Estimation of the statistical error in large eddy simulation results, 15–19 July 2002, Wageningen. American Meteorological Society, Boston, p 3.12
Monin AS, Oukhov AM (1954) Osnovnye zakonomernosti turbulentnogo peremesivanija v prizemnom sloe atmosfery (Basic laws of turbulent mixing in the atmosphere near the ground). Trudy Geofiz Inst AN SSSR 24(151):163–187
Neftel A, Spirig C, Ammann C (2008) Application and test of a simple tool for operational footprint evaluations. Environ Pollut 152:644–652
Paulson CA (1970) The mathematical representation of wind speed and temperature profiles in the unstable atmospheric surface layer. J Appl Meteorol 9:857–861
Panofsky HA (1984) Vertical variation of roughness length at the Boulder atmospheric observatory. Boundary-Layer Meteorol 28:305–308
Panofsky HA, Tennekes H, Lenschow DH, Wyngaard JC (1977) The characteristics of turbulent velocity components in the surface layer under convective conditions. Boundary-Layer Meteorol 11:355–361
Prueger JH, Kustas WP, Hipps LE, Hatfield JL (2004) Aerodynamic parameters and sensible heat flux estimates for a semi-arid ecosystem. J Arid Environ 57:87–100
Raupach MR (1994) Simplified expressions for vegetation aerodynamic roughness length and zero-plane displacement as functions of canopy height and area index. Boundary-Layer Meteorol 71:211–216
Rotach MW (1994) Determination of the zero plane displacement in an urban environment. Boundary-Layer Meteorol 67:187–193
Schmid HP (1994) Source areas for scalars and fluxes. Boundary-Layer Meteorol 67:293–318
Schotanus P, Nieuwstadt FTM, de Bruin HAR (1983) Temperature-measurement with a sonic anemometer and its application to heat and moisture fluxes. Boundary-Layer Meteorol 26:81–93
Takagi K, Miyata A, Harazono Y, Ota N, Komine M, Yoshimoto M (2003) An alternative approach to determining zero-plane displacement, and its application to a lotus paddy field. Agric For Meteorol 115:173–181
Toda M, Sugita M (2003) Single level turbulence measurements to determine roughness parameters of complex terrain. J Geophys Res 108(D12):4363
Tsai JL, Tsuang BJ, Lu PS (2010) Measurements of aerodynamic roughness, Bowen ratio, and atmospheric surface layer height by eddy covariance and tethersonde systems simultaneously over a heterogeneous rice paddy. J Hydrometeorol 11:452–466
van Dijk A, Moene AF, de Bruin HAR (2004) The principle of surface flux physics: theory, practice and description of the ECPACK library. Internal report 2004/1. Meteorology and Air Quality Group, Wageningen University, Wageningen, The Netherlands, 99 pp
van de Boer A, Moene AF, Schüttemeyer D, Graf A (2013) Sensitivity and uncertainty of analytical footprint models according to a combined natural tracer and ensemble approach. Agric For Meteorol 169:1–11
Weaver HL (1990) Temperature and humidity flux–variance relations determined by one-dimensional eddy correlation. Boundary-Layer Meteorol 53:77–91
Wieringa J (1993) Representative roughness parameters for homogeneous terrain. Boundary-Layer Meteorol 63:323–363
Wilczak JM, Oncley SP, Stage SA (2001) Sonic anemometer tilt correction algorithms. Boundary-Layer Meteorol 99:127–150
Zhang HS, Park SU (1999) Comments on 'A new method to determine the zero-plane displacement'. Boundary-Layer Meteorol 91:135–139